

Designing a High Performance Electroless Nickel and Immersion Gold to Maximize Highest Reliability

Robert Spreemann
Rick Nichols
Sandra Nelle

Atotech Deutschland GmbH
Berlin, Germany
Robert.spreemann@atotech.com
Rick.nichols@atotech.com
Sandra.nelle@atotech.com

ABSTRACT

The latest highest reliability requirements demand a high performance electroless nickel and immersion gold (HP ENIG). The new IPC specification 4552A has refocused the industry with reference to nickel corrosion. The interpretation of the existing specification, that judges corrosion on 3 levels, is complex and if misinterpreted can lead to phantom failures. An obvious way to avoid any potential misinterpretation is to eradicate any evidence of corrosion completely.

Solderability and environmental corrosion resistance are also highly significant prerequisites when discussing Highest Reliability. These will be evaluated by High Speed Shear testing (HSS) and gas chamber testing respectively. In addition to the more demanding requirements of the HP ENIG to satisfy High Reliability requirements, the system needs to exhibit good basic layer characteristics.

It is also the intention of this paper to evaluate whether there is any 'value added' or unintended benefits to a HP ENIG. An example of this would be superior gold distribution and associated gold saving potential. Data generated by Design of Experiment (DOE) will be used to evaluate the impact of electroless nickel variables in combination with traditional and cyanide free immersion gold on recognized quality expectations. The results are expected to be practical and production applicable solution underpinned by solid data and it is hoped that they may dispel myths or misunderstandings within the printed circuit board (PCB) manufacturing environment.

Key words: Highest reliability, Nickel corrosion, Corrosion resistance, Solderability, Black pad

ASR	As received
ENIG	Electroless Nickel Immersion Gold
BS	Ball Shear
CBP	Cold Ball Pull
CN	Cyanide
CNF	Cyanide-free
CV	Coefficient of Variation
DOE	Design of Experiments
HP	High-Phosphorous
MAG	Magnification
MP	Mid-Phosphorous
MPF	Mid-Phosphorous Flex
Ni	Nickel
NSS	Neutral Salt Spray
P	Phosphor
PCB	Printed Circuit Board
SEM	Scanning Electron Microscope
SST	Solder Spread Test
T	Temperature

INTRODUCTION AND BACKGROUND

PCBs are an integral part of many electronic devices. The demand for more versatile and powerful devices is critically affecting the size of such devices resulting in tougher requirements for the PCB manufacturer. Besides the steady reduction of solder contacts, electronic devices are also more often used at higher operating temperatures [1] as well as in more harsh environmental conditions. Therefore, thermal stability of the solder joint as well as corrosion resistance are becoming more and more important[1], thus creating a demand for a high performance ENIG. Namely, a specially designed process using high phosphorous electroless nickel (> 9.5-13% wt% P) and immersion gold as final finish [2].

Unfortunately, several studies argue that a higher phosphorous content in the Ni layer should result in worse layer qualities compared to a mid-phosphorous Ni layer. Amongst other things it was claimed that the wetting on Ni phosphorous degrades with increasing phosphorous content [3]. Or that shear strength of solder joints should decrease due to the appearance of a P-rich layer at the joint interface [4] along with a higher occurrence of brittle fractures at the Ni-Sn interface [5]. Therefore, the goal of this paper will be to disprove outdated data and to show that HP ENIG can fulfill highest requirements in solderability, solder joint reliability, bondability and corrosion resistance.

METHODS, MATERIALS AND EXPERIMENTAL

Materials and Cleaning

The test vehicles used were fabricated by a PCB manufacturer. The substrates were cleaned via a wet chemical approach before ENIG.

ENIG coating and process flow

The process flow is displayed in Figure 1.



Figure 1: Schematic drawing of ENIG process flow

The cleaned Cu surface was activated by a palladium catalyst and plated in a Mid-P electroless Ni bath as well as a High-P electroless Ni bath. The last process step was immersing the test boards with High-P Ni layer into a cyanide free Au bath (CNF Au) and the test board with Mid-P Ni layer into a conventional cyanide containing Au bath (CN Au). The thickness of the Nickel and Gold is controlled in the range of 4-6 μm nickel and 40-60 nm gold.

Measurement tools and methods

The thickness uniformity of the Nickel and Gold layer was investigated by X-ray fluorescence measurement (XRF). The cross section samples were prepared by epoxy casting, grinding and polishing. The samples were investigated by optical microscopy and scanning electron microscopy (SEM).

The equipment for aluminum wire bond testing used was a production automatic wedge/wedge-bonder with aluminum (AlSi 1%) wires from a materials supplier at a diameter of 25 μm and a break load of approx. 15 g. The production pull tester used a pull speed of 500 $\mu\text{m/s}$. The number of pulls per sample was 30. The parameter settings used in the bond of the two wedges can be read from Table 1.

Table 1: Parameter settings used for wire bond tests

Parameter	First Bond	Second Bond
US-Power [a.u.]	90	90
US-Time [ms]	25	25
Bond Force [cN]	20	25

The test and ball soldering conditions for the cold ball pull test and ball shear test are the following. The solder balls used were of SAC 305 alloy. The ball diameter is 450 μm . Flux used is of a production Tacky Flux type. The reflow profile is sketched in Figure 2.

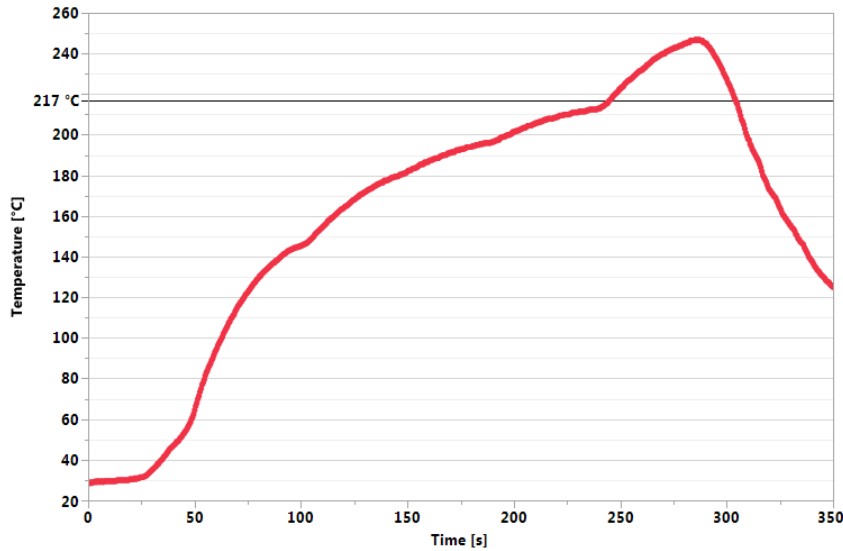


Figure 2: Linear lead-free reflow profile used for cold ball pull and ball shear test; peak-T: 250°C

A production reflow oven was used for all soldering tests. Reflow was done under nitrogen atmosphere for cold ball pull, ball shear and high speed shear testing. For the tests, production test boards with solder mask defined (SMD) ball grid arrays (BGA) with a solder resist opening (SRO) of 380 μm were used. The settings for cold ball pull, ball shear and high-speed shear test can be found in Table 2.

Table 2: Settings used for cold ball pull, ball shear and high speed shear test.

Test	Cartridge	Speed	Height	Delay Time	No. of Balls
Cold Ball Pull	5kg	5 mm/s	-	3-4 h	30
Ball Shear	5kg	210 $\mu\text{m/s}$	50 μm	4 h	30
High Speed Shear	Cartridge	0.6 m/s	20 μm	4 h	20

In addition, solder indicator (SI) and solder spread tests (SST) were performed. In these cases a solder paste production printer was used with a production solder paste. The Reflow atmosphere was air with the following reflow profile:

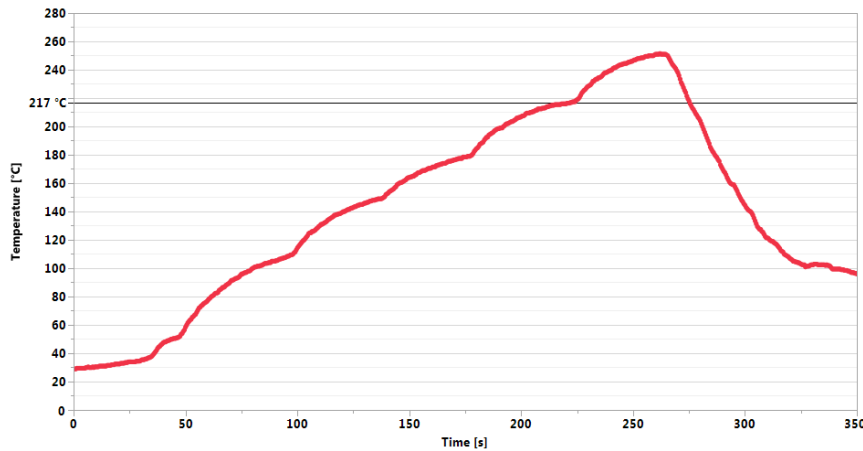


Figure 3: Lead-free reflow profile used for solder indicator and solder spread test; peak-T: 248°C

For the solder spread test the stencil diameter was 1000 μm with the number of dots being 5. A production type optical microscope was used for the evaluation.

For selective wave soldering tests, a production type selective wave soldering machine used, with the following settings (Table 3). The tested PCB thickness was 1.5 mm and a production type optical microscope was used for the evaluation.

Table 3: Settings used for selective wave soldering.

Solder	SAC 305
Flux	Production type
Size of solder nozzle	18 mm inside; 20 mm outside
Solder temperature	280°C
Flux dosage	30%
Fluxing speed	25 mm/s
Soldering speed	6 mm/s

The neutral salt spray test was conducted according to ISO 9227:2006.

RESULTS / DISCUSSION

Au thickness distribution and plating rate

Having a uniform Au thickness is beneficial for commercial application because it allows cost savings due to lower minimum gold thicknesses which have to be deposited. PCB manufacturers maybe concerned that a high phosphorous Ni is not able to achieve the gold distributions they are used to from mid phosphorous Ni. This is because it is perceived that the more noble properties of a High-P Ni can affect the Au deposit qualities. In order to show that one can deposit Au with the same distribution also on top of a High-P layer, a proprietary thickness distribution test board with different pad sizes (Figure 4) was plated and afterwards measured by XRF.

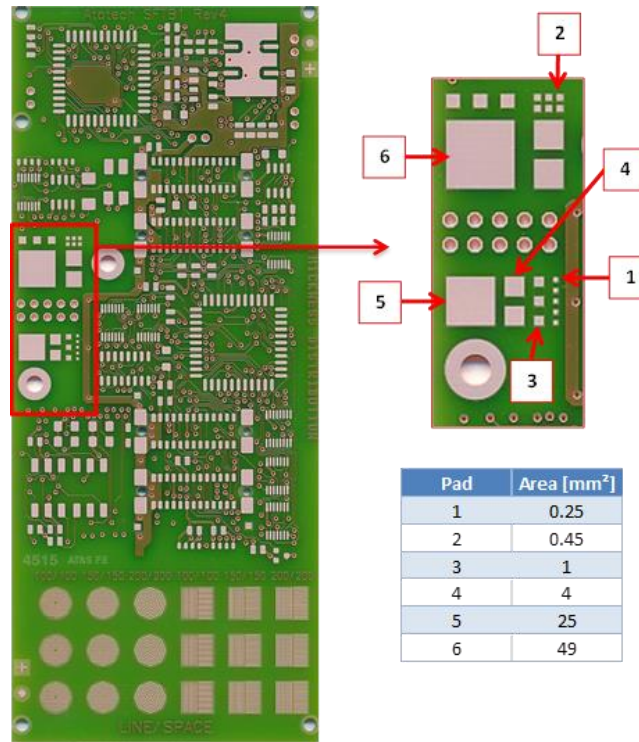
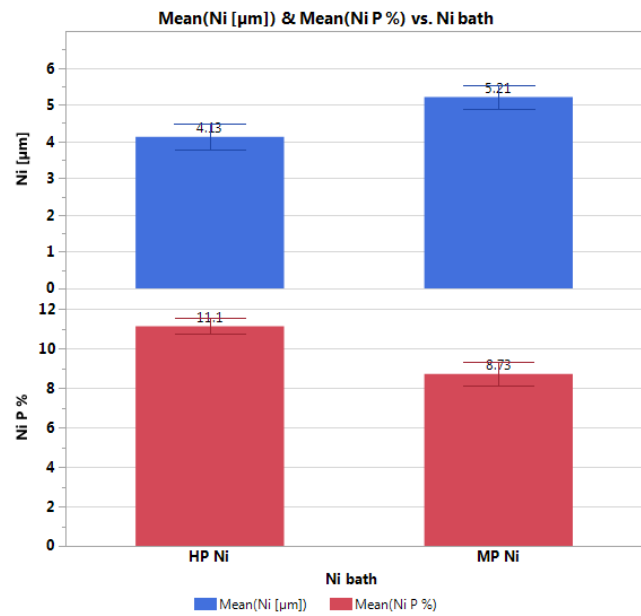
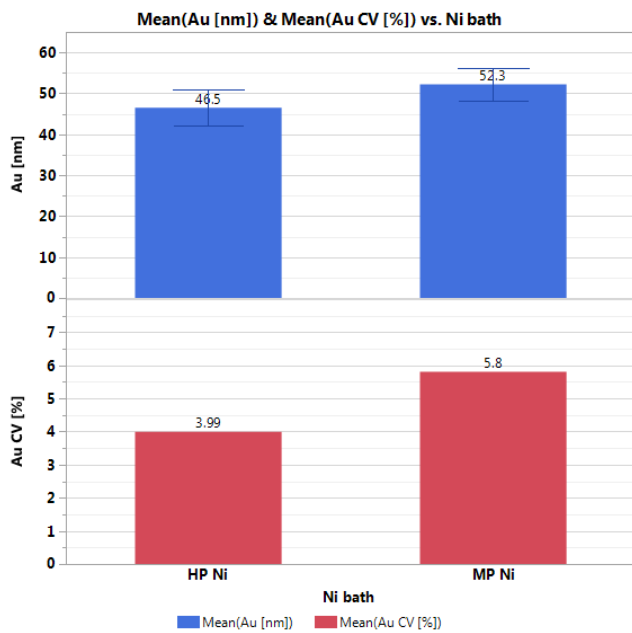


Figure 4: Company test board thickness distribution, measured pads and pad size.

The results can be seen in Figure 5. Depositing similar Au thicknesses with the cyanide free Au bath on High-P Ni and conventional cyanide containing Au bath on Mid-P Ni resulted in similar or perhaps even slightly better Au thickness distribution for the High-P Ni layer and the cyanide free Au bath. In addition to the Au thickness also the Ni thickness as well as the P-content of the Ni layers is displayed.



a) Au thickness and standard deviation.

b) Ni thickness and P-content.

Figure 5: XRF measured mean Au thickness as well as coefficient of variation (CV) over different pad sizes, Ni thickness and P-content on company thickness distribution test board for Mid-P Ni and High-P Ni.

Solderability

The solder indicator test is used to measure the wetting behavior as a function of the distance between the printed solder paste (Figure 6). The scale ranges from 1 to 10 points (bottom to top in Figure 6) with 10 being the best and indicating excellent wetting.

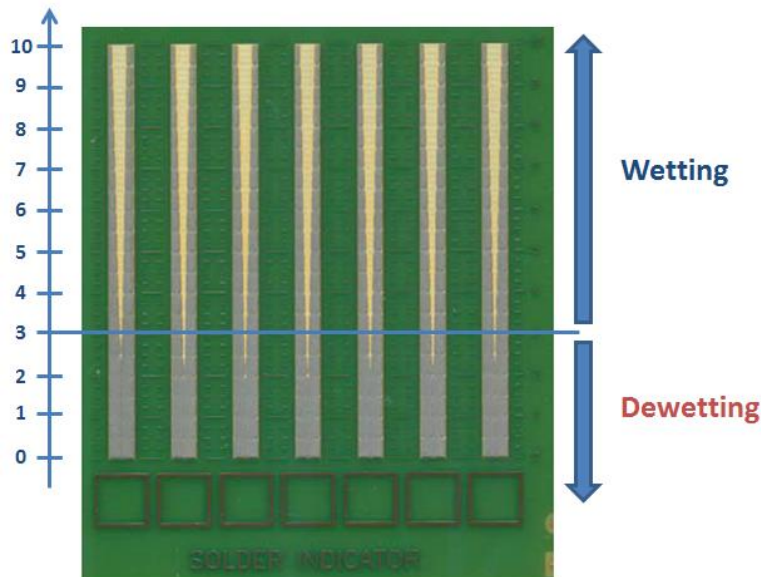


Figure 6: Solder indicator test board with solder paste.

After printing, the test boards are heated in the oven and the solder paste should converge and one can read of the result from the scale. The findings of this test can be found in Figure 7.

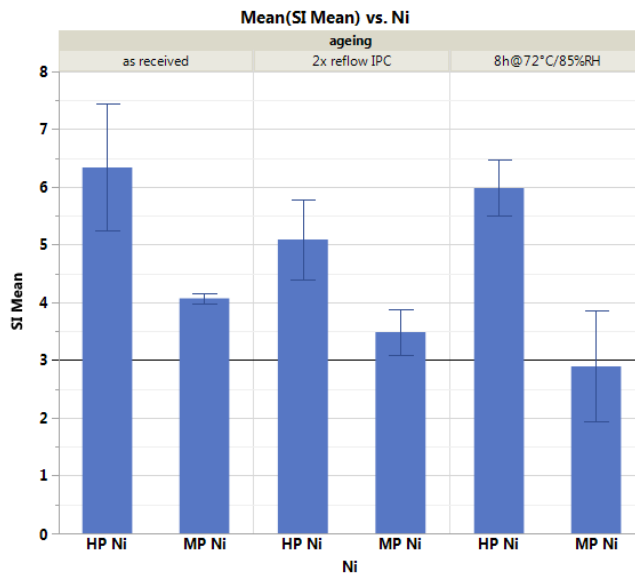


Figure 7: Results solder indicator test for Mid-P and High-P Ni and different aging conditions.

One can see very good wetting behavior for High-P Ni (far beyond minimum pass criteria of 3) across all aging conditions compared to Mid-P Ni for similar Au thickness.

Another way to measure the wettability of the Ni/Au layer is the solder spread test. In this test, a solder dot is printed in the middle of a circular pad (Figure 8).

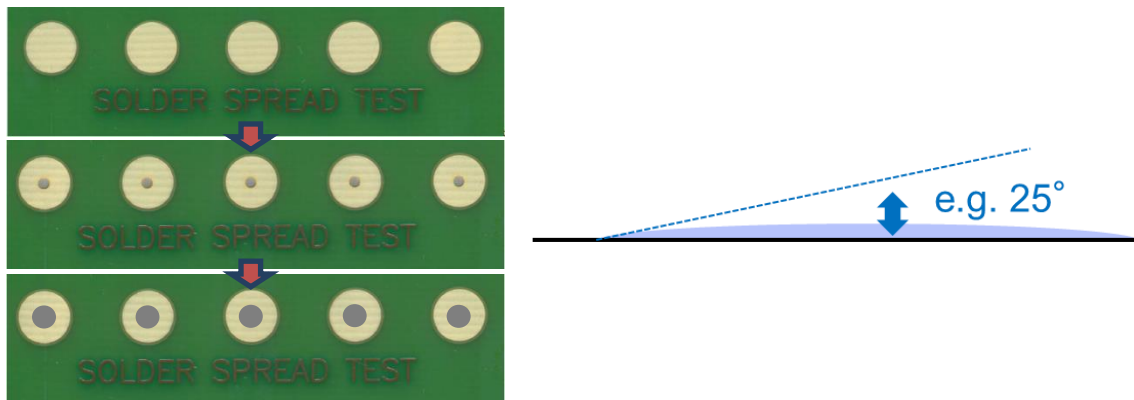


Figure 8: Solder spread test area with (bottom) and without (top) printed solder paste.

During reflow of the test board, the dot is melting, and one can measure the wetting angle between the solder and the Au layer afterwards. This gives an indication of the wetting behavior of the layer. The results of the solder spread tests are displayed in Figure 9.

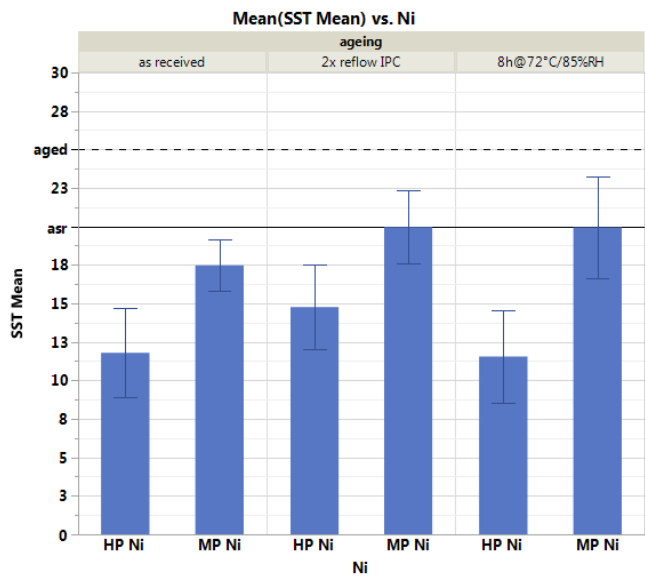


Figure 9: Results of solder spread test for Mid-P and High-P Ni and different aging conditions.

Regarding the solder spread test a lower number means a better wetting. Therefore, like in the SI test the HP ENIG system is showing a significantly better wettability across all aging conditions. The last test which gives information about wettability is the selective wave soldering. In this test one side of the test board is soldered (Figure 10) and afterwards it is checked if the solder was able to wet the PTHs completely (Figure 11).

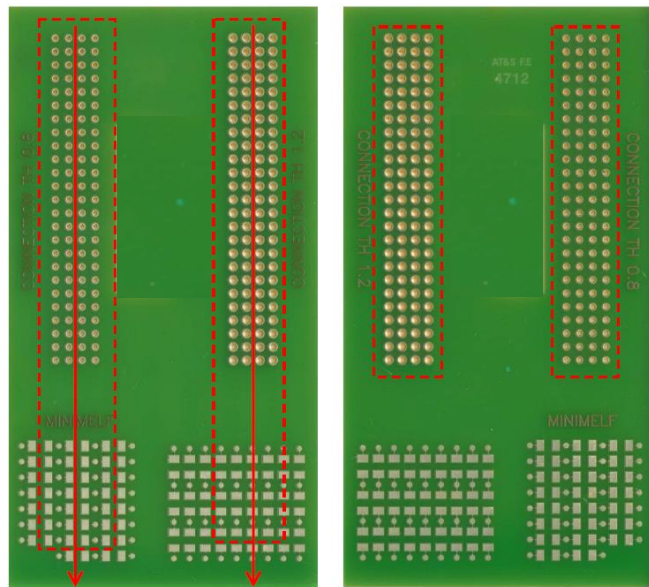


Figure 10: Selective wave test area on standard company test board. Solder contact site (left) and evaluating site (right).

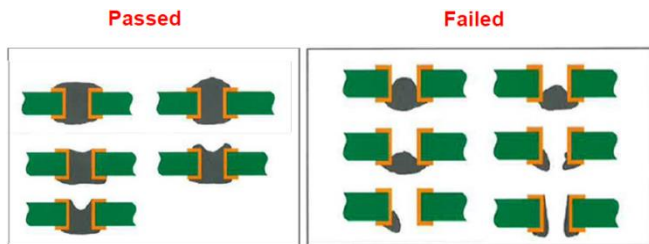


Figure 11: Pass and fail criteria of selective wave test.

Looking at Figure 12, one can see the selective wave test results for Mid-P and High-P Ni ENIG systems. Again, like in both soldering tests before the High-P Ni shows significantly better solderability across all aging conditions compared to Mid-P

Ni. The overall better solderability of the High-P Ni compared to Mid-P Ni may be explained by referring to the following report [6].

This report mentioned that the entrapment of bath residues due to corrosion and also the exposure of the Ni surface to oxidation are responsible for the surface to become non-wettable. Using a High-P Ni layer should therefore reduce the occurrence of these two possible causes by being more corrosion/oxidation resistant than Mid-P Ni layers. Furthermore, in order to achieve similar wetting results also for MP ENIG system, higher Au thicknesses, at the risks of stronger corrosion, would be necessary. Therefore, HP ENIG offers a huge cost advantage due to less gold consumption while still exhibiting excellent solderability.

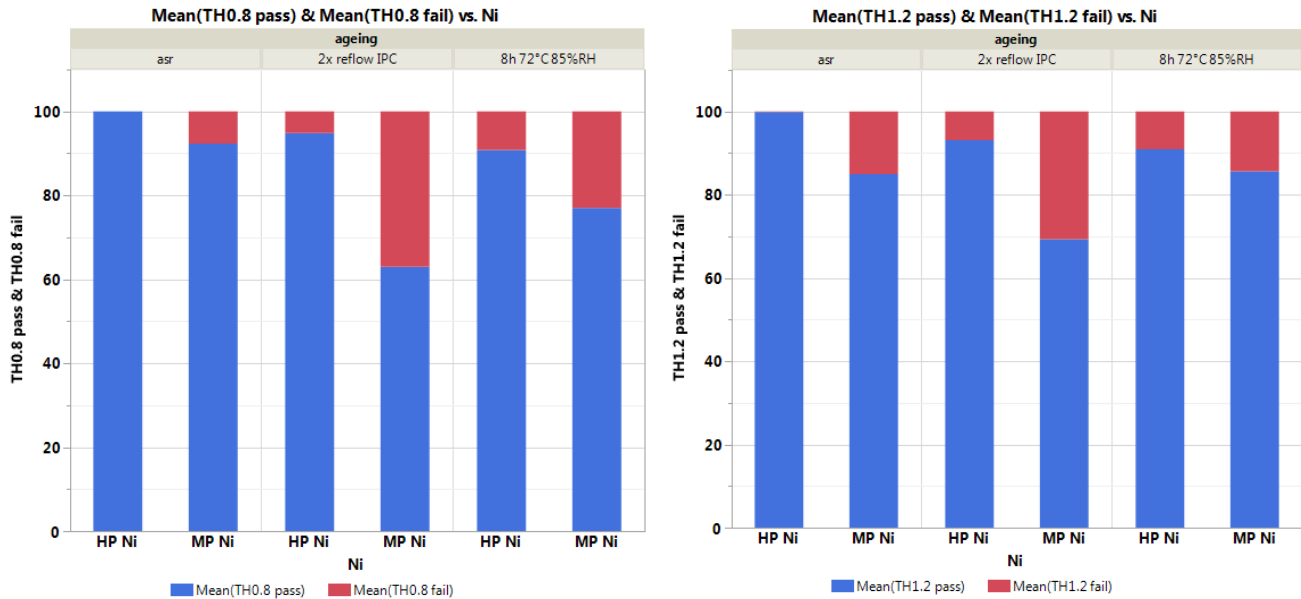


Figure 12: Results of selective wave soldering for different PTH sizes (0.8 and 1.2 mm diameter).

Reliability tests

The reliability of a solder joint can be examined for example by ball shear, cold ball pull and also high speed shear test. In this study all three above mentioned reliability tests were conducted in order to find differences between the tested ENIG layer systems. The ball shear test uses a tool to shear off the solder balls at a defined height as well as defined speed. The force needed to pull of the solder ball is measured. Furthermore, also the fracture mode is recorded to check for brittle solder joints. The cold ball pull test instead is using a claw to pull off the solder ball from the substrate in a vertical direction and the pull strength until failure is measured. The high-speed shear test is, as the name suggests, a faster version of the normal ball shear test but in addition to the ball shear test also the total energy needed to pull of the solder ball is recorded.

The shear strength as well as the fracture mode for the ball shear test can be seen in Figure 13. Furthermore, a classification of the fracture mode can be seen in Figure 14. As long as ball shear test is concerned no difference between Mid-P and High-P Ni was found. Both Ni bath types exhibit good shear strength as well as a good fracture mode with up to no intermetallic fractures.

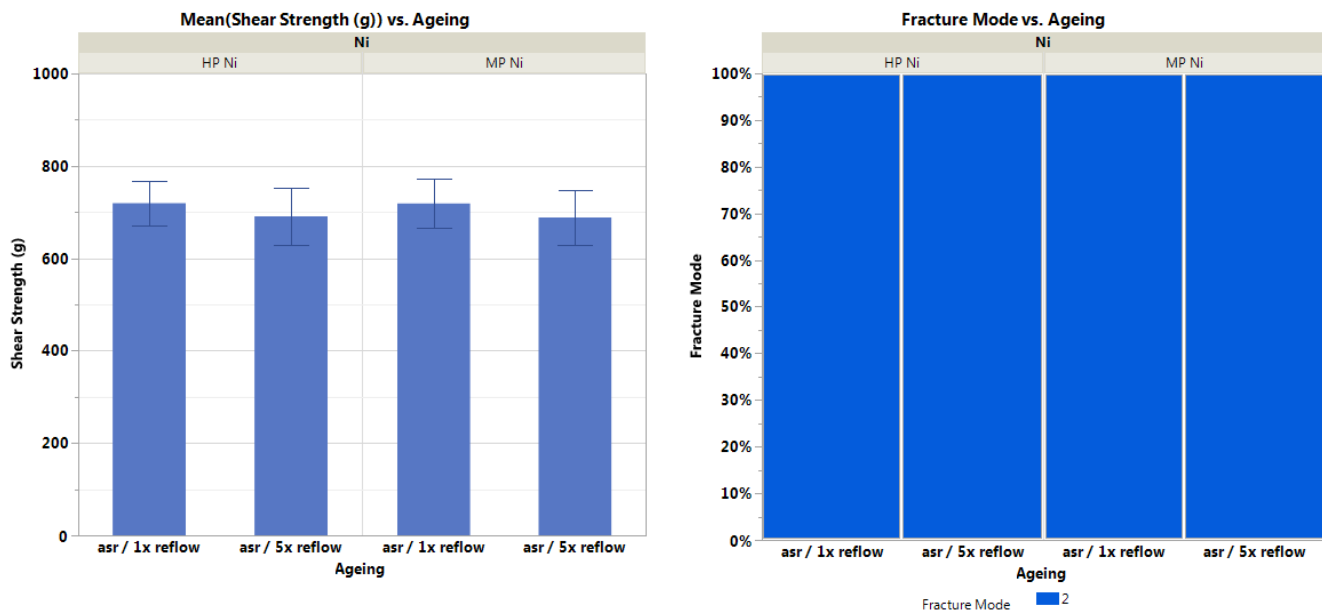


Figure 13: Shear strength (top) and fracture mode (bottom) of ball shear test for different Ni baths and aging conditions.

Mode 1	Pad pull-out
Mode 2	Intermetallic fracture < 5%
Mode 3	Intermetallic fracture < 25%
Mode 4	Intermetallic fracture < 95%
Mode 5	Intermetallic fracture > 95%

Figure 14: Fracture mode classification for ball shear test.

Looking at the pull strength of the cold ball pull test (Figure 15, left) again no difference can be seen for Mid-P Ni and High-P Ni, but although pull strengths are similar there are significant differences regarding the fracture modes of the respective Ni layer (Figure 15, right). The fracture modes of the Mid-P layer tend to be more brittle compared to the fracture modes of the High-P Ni (Figure 16).

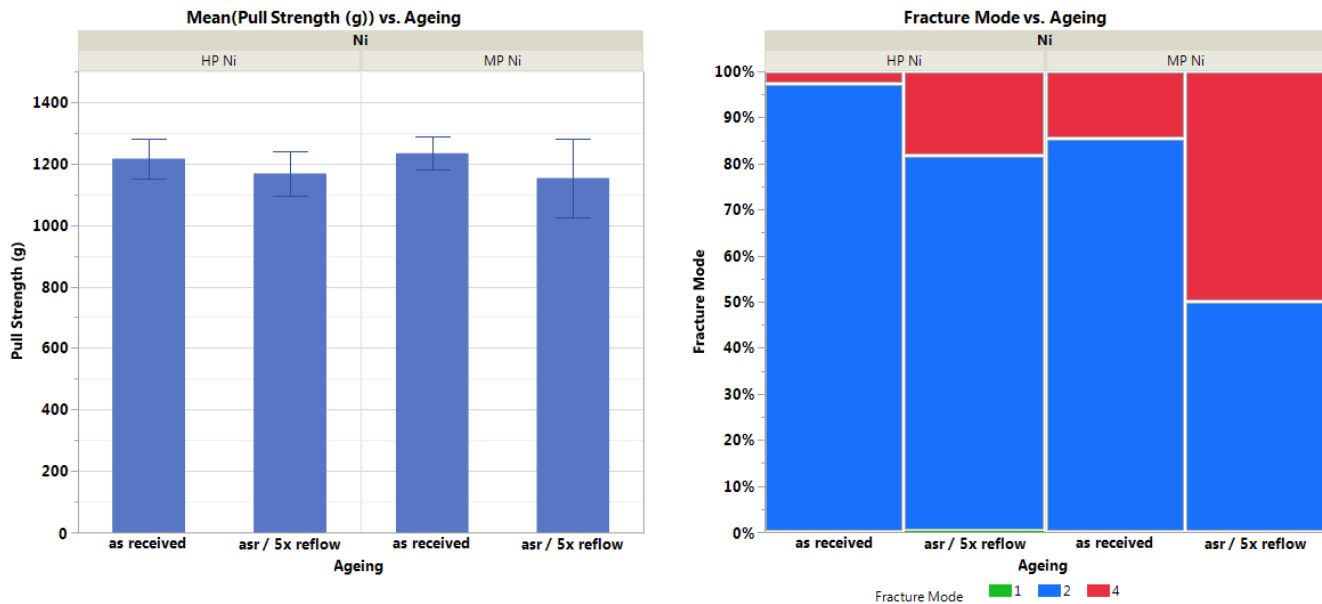


Figure 15: Pull strength (top) and fracture mode (bottom) of cold ball pull test for different Ni baths and aging conditions.

Mode 4	Bond failure		Process or material problems
Mode 3	Ball extruded		Jaw cavity too big, jaw closing force too low or very soft solder.
Mode 2	Ball failure		Good bond. Maximum test force possible or jaw cavity too small.
Mode 1	Pad failure		Good bond. Possible pad design problem.
Mode 0	Mixture of Mode 1 and Mode 4		

Figure 16: Fracture mode classification for cold ball pull test.

Similar trends as in cold ball pull can also be seen in high speed shear test (Figure 17). In as received (asr) / 1x reflow condition both Ni layers show the same total energy and similar fracture modes (Figure 17 (right) and Figure 18). But after asr / 5x reflow the total energy as well the fracture modes got significantly worse for the Mid-P Ni layer compared to the High-P Ni layer.

This difference in fracture modes for cold ball pull as well as high speed shear between Mid-P Ni and High-P Ni may be related to different kind of intermetallic compound (IMC) formation. It is known that IMC formation and Ni dissolution are affected by P-content in the Ni layer. Electrolytic Ni (no codeposited phosphor) is showing a much faster Ni dissolution into the solder as well as a faster IMC growth compared to electroless Ni [7].

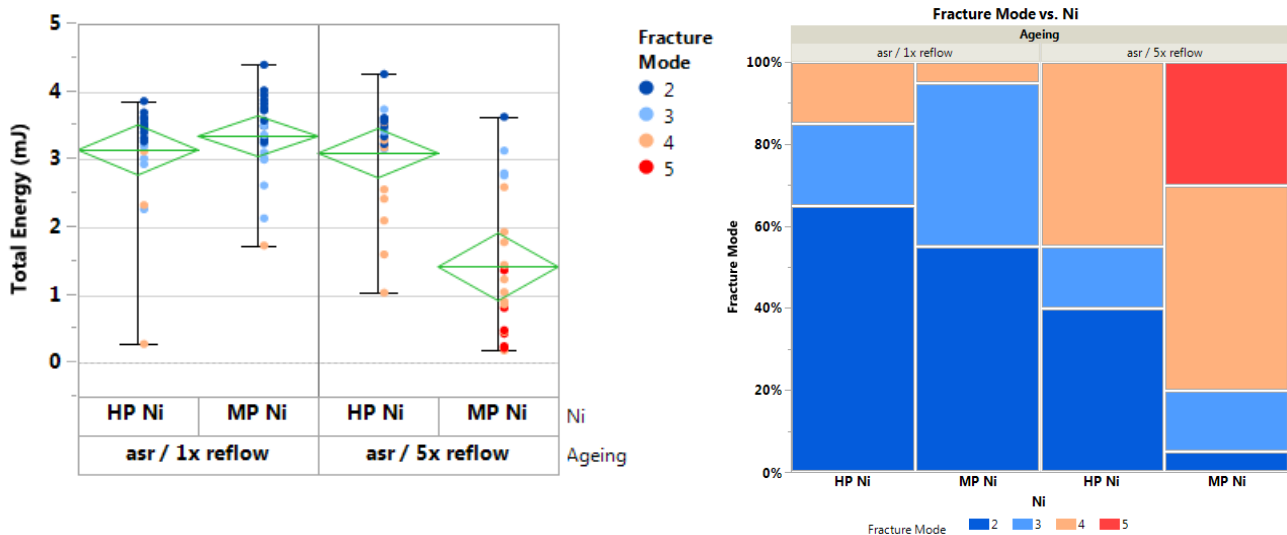


Figure 17: Total energy (left) and fracture mode (right) of high speed shear test for different Ni bathes and aging conditions (0.2 m/s shear speed, 20 μ m shear height).

Mode 1	Pad pull-out
Mode 2	Intermetallic fracture < 5%
Mode 3	Intermetallic fracture < 25%
Mode 4	Intermetallic fracture < 95%
Mode 5	Intermetallic fracture > 95%

Figure 18: Fracture mode classification for high speed shear test.

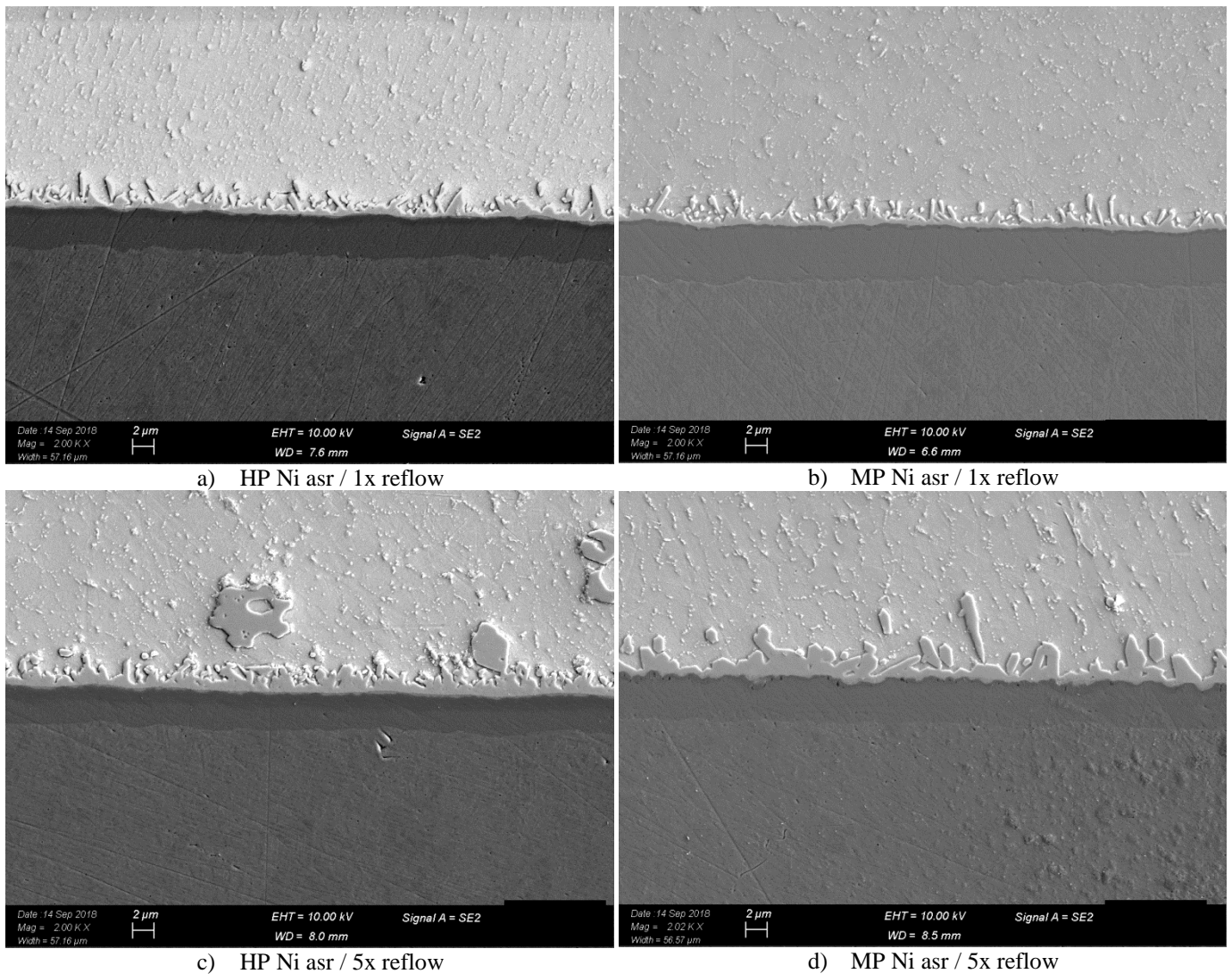


Figure 19: SEM cross sections (2000x) of printed solder balls for High-P Ni (left) and Mid-P (right) for 1x reflow as well as 5x reflow.

This is supported by SEM cross section pictures of the attached solder balls. In Figure 19 one can see an overview of the IMC for HP and MP Ni in asr / 1x reflow as well as asr / 5x reflow condition. Regarding 1x reflow condition MP and HP Ni are showing a similar needle like IMC growth. After 5 x reflow both Ni layer types exhibit an IMC growth, but the structure of the IMC changed. The IMC of the High-P Ni still consists of needle like structures but for MP the structure changed to a more nodule like IMC. Having a more detailed look at the IMCs for MP and HP Ni (Figure 20) one can see a distinct dark band directly underneath the IMC for the MP Ni. This dark band is a phosphor enriched layer which is growing and getting porous with increasing reflow cycles whereas for the HP layer one can only see some kind of gradient indicating the enrichment of phosphorus in the Ni layer. Maybe this distinct growing and porous phosphor enriched layer is responsible for the degrading fracture modes of the MP Ni with increasing reflow cycles.

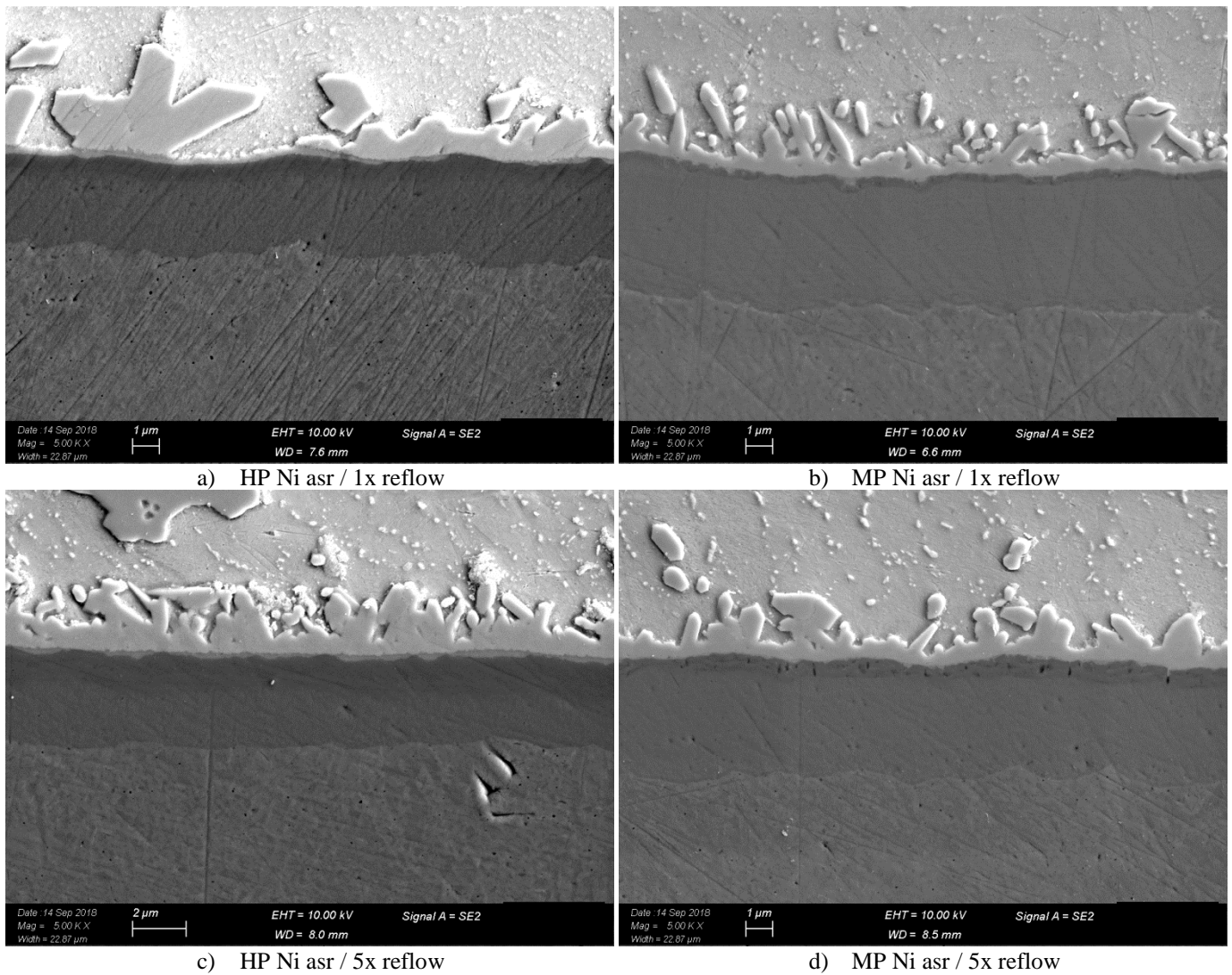


Figure 20: Detailed SEM cross sections (5000x) of printed solder balls for High-P Ni (left) and Mid-P (right) for 1x reflow as well as 5x reflow.

Bondability

For aluminum wire bonding tests, two wedge ends were bonded by ultrasonic to the surface of the substrate. After this, a wire pull test was conducted, pulling from the middle of the wire and recording pull strength as well as fracture mode. For aluminum wire bonding maybe, one can expect different behavior because the wedges are bonded to surfaces with different hardness. But as can be seen in Figure 21 (left) both Ni layers were able to surpass the minimum mean pull strength criteria of 7.5g break load easily.

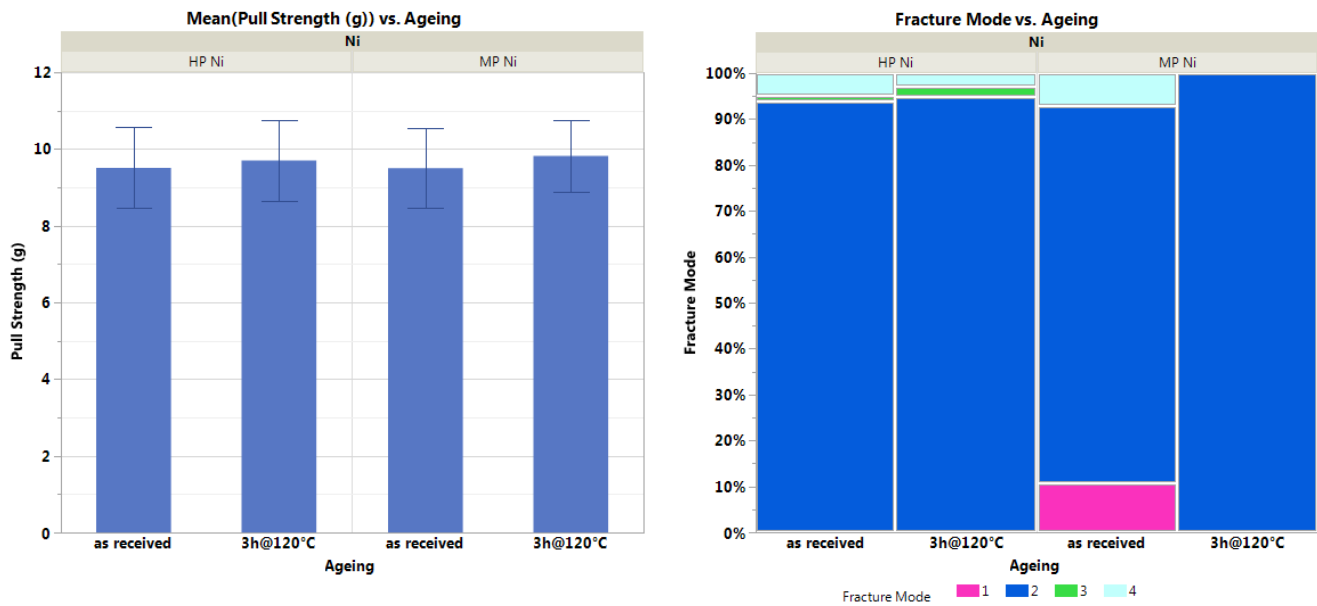


Figure 21: Pull strength and fracture mode of aluminum wire bonding for different Ni layers and ageing conditions.

High-P Ni has a lower hardness (Figure 23) and also a lower surface roughness than Mid-P Ni (Figure 24). Both factors are playing a key role in bondability, because thin Au layers are following the contours of the underlying Ni surface [8].

This may be a reason why the fracture modes for High-P Ni layer are slightly better than the fracture modes of the Mid-P Ni layer.

Mode 1	Wedge lift first bond
Mode 2	Neck break first bond
Mode 3	Wire loop break
Mode 4	Neck break second bond
Mode 5	Wedge lift second bond

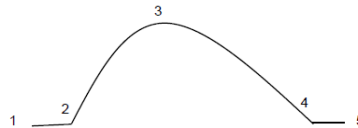


Figure 22: Fracture mode classification for Al wire bonding.

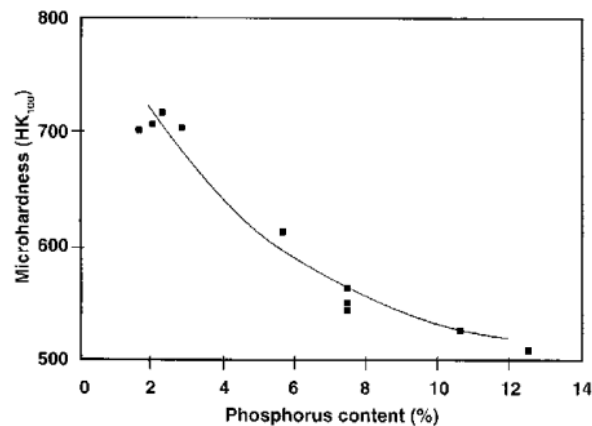


Figure 23: Hardness of the Ni layer as a function of phosphorous content [9].

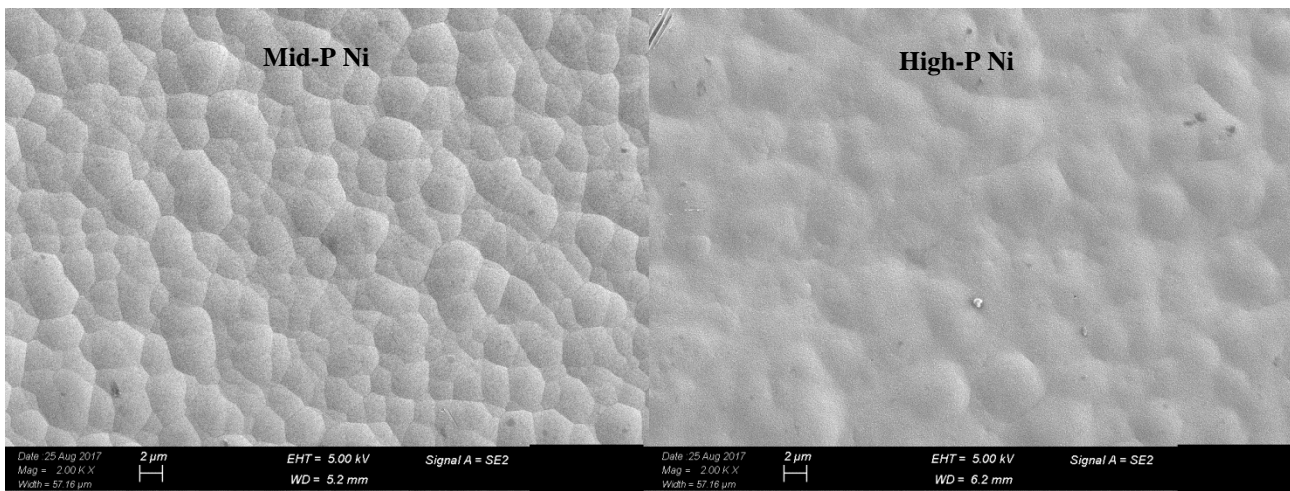


Figure 24: SEM surface pictures of Mid-P and High -P Ni layers.

Corrosion

With the new IPC specification 4552A about to be released, corrosion has come into the spotlight for the PCB industry. Corrosion can happen either by applying the immersion Au bath on the Ni layer and/or by any kind of corrosive environment. Therefore, the thickness of the deposit as well as the porosity is of great importance to corrosion resistance of the final ENIG system. Applying high phosphorous Ni reduces the tendency of the deposit to be porous which leads to a higher corrosion resistance. Further advantages of the amorphous high phosphorous deposits are:

1. Less to no grain boundaries at which corrosion can be initiated
2. They tend to form passive, glassy surfaces which provide added protection [9]

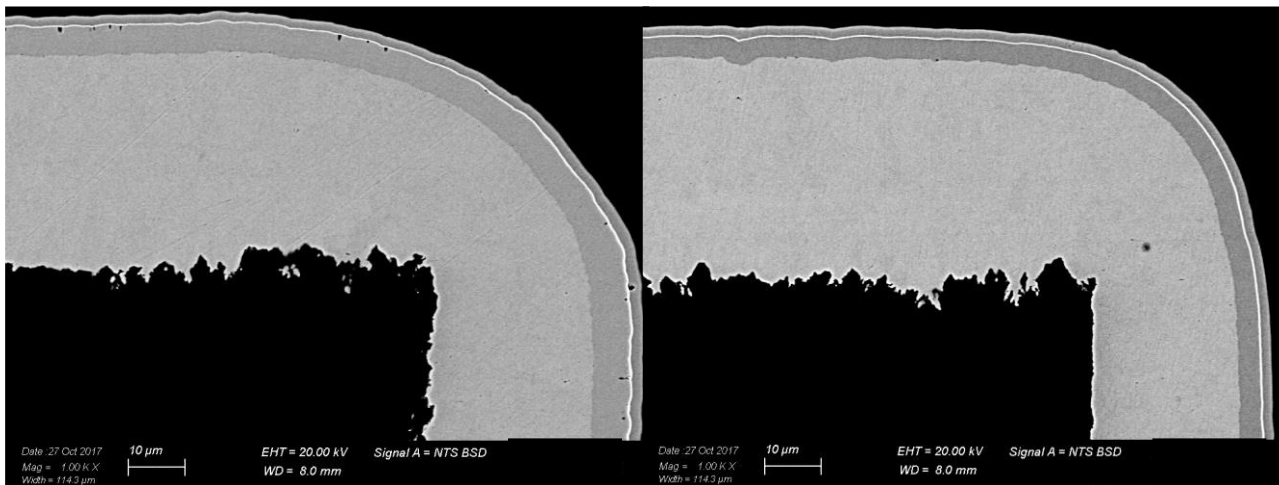


Figure 25: Exemplary SEM cross section pictures (1000xMAG) of Mid-P Ni (left) and High-P Ni (right).

In order to compare Mid-P and High-P nickel layers (examples see Figure 25) regarding the corrosive attack by the immersion Au bath, both ENIG systems were evaluated according to IPC 4552A. As can be seen in Figure 26, High-P Ni offers a better corrosion performance and thus leaves no room for misinterpretation.

	MP Ni	HP Ni
PTH	Level	Level
Location 1	1	0
Location 2	3	0
Location 3	1	0
Location 4	1	0
Location 5	1	0
Location 6	1	0
Location 7	1	0

	Total Count	Total Count
Level 0	0	7
Level 1	6	0
Level 2	0	0
Level 3	1	0

Product Rating	1	0
	1	0

Figure 26: IPC corrosion evaluation according to IPC 4552A for Mid-P and High-P Ni.

The neutral salt spray (NSS) test is one of many methods to determine the corrosion resistance of an ENIG layer system in a corrosive environment. The conditions of this test are forcing an accelerated corrosion attack which can give indications about the corrosion resistance of the respective sample. The results for the NSS test can be found in Table 4. Because of the aggressive nature of this test, both ENIG systems show corrosion but the ENIG with HP Ni was able to withstand the corrosive attack better than the MP ENIG because of the higher phosphorous content in the Ni layer. This result is making the HP ENIG the better solution for PCBs which have to function in a corrosive environment.

Table 4: Results Neutral Salt Spray test up to 144h for MP ENIG and HP ENIG.

	asr	24h	48h	96h	144h
ENIG (MP)					
ENIG (HP)					

CONCLUSIONS

It was the goal of this paper to overcome myths and misunderstandings within the PCB manufacturing environment regarding the HP ENIG finish. It could clearly be shown that HP ENIG offers significantly better solderability than MP ENIG for similar gold layer thickness which can result in huge cost advantages for HP ENIG because thinner Au layers can be applied with the same qualities as standard MP ENIG. In addition, HP ENIG also offers a great solder joint reliability performance especially after multiple reflow cycles, possibly due to its decreased nickel dissolution and different IMC growth compared to MP ENIG. The lower hardness and surface roughness of HP Ni also seems to positively influence aluminum wire bonding fracture mode performance. Finally, the amorphous structure as well as the electrochemically more noble behavior of the HP Ni is making it the best choice for exposure to corrosive media, either immersion Au baths and/or corrosive environment.

ACKNOWLEDGEMENTS

The authors would like to acknowledge KSG Leiterplatten GmbH who fabricated the proprietary test vehicles used in this study.

REFERENCES

- [1] S. Nieland, "Einfluss des Phosphors auf die Phasenbildung und das Phasenwachstum bei chemisch abgeschiedenen Ni/P-Bumps und schablonengedruckten Mikrolotkontakten," Fakultät III - Prozesswissenschaften Bereich Werkstoffwissenschaften der Technischen Universität Berlin, Berlin, 2002.
- [2] K. J. H. R. D. H.-J. S. Sven Lamprecht, "Impacts of Bulk Phosphorous Content of Electroless Nickel Layers to Solder Joint Integrity and their Use as Gold- and Aluminum-Wire Bond Surface," Atotech, 2004.
- [3] S. K. L. A. S. Mei Z, "A Failure Analysis and Rework Method of Electronic Assembly on Electroless Ni/Immersion Au Surface Finish," in *SMTA International*, Chicago, 1999.
- [4] Y. C. C. K. N. T. M. O. Alam, "Effect of reaction time and P content on mechanical strength of the interface formed between eutectic Sn-Ag solder and Au/electroless Ni(P)/Cu bond pad," *Journal of Applied Physics*, vol. 94, no. 6, pp. 4108-4115, 2003.
- [5] P. A. M. R. P. Snugovsky, "Electroless Ni/Immersion Au Interconnects: Investigation of Black Pad in Wire Bonds and Solder Joints," *Journals of Electronic Materials*, vol. 30, no. 9, pp. 1262-1270, 2001.
- [6] P.-E. Tegehall, "Review of the Impact of Intermetallic Layers on the Brittleness of Tin-Lead and Lead-Free Solder Joints," IVF Project Report, 2006-2007.
- [7] Y. C. Ahmed Sharif, "Interfacial reactions on electrolytic Ni and electroless Ni(P)," *Journal of Alloys and Compounds*, vol. 393, pp. 135-140, 2005.
- [8] G. Harman, "Wire Bonding in Microelectronics," McGraw Hill, 2010, pp. 183-223.
- [9] R. Parkinson, *Properties and applications of electroless nickel*, Nickel Development Institute.